

Theory of Magnetic Field Induced Spin Density Wave in High Temperature Superconductors

Yan Chen and C. S. Ting

Texas Center for Superconductivity and Department of Physics, University of Houston, Houston, TX 77204

The induction of spin density wave (SDW) and charge density wave (CDW) orderings in the mixed state of high T_c superconductors (HTS) is investigated by using the self-consistent Bogoliubov-de Gennes equations based upon an effective model Hamiltonian with competing SDW and d -wave superconductivity interactions. For optimized doping sample, the modulation of the induced SDW and its associated CDW is determined by the vortex lattice and their patterns obey the four-fold symmetry. By decreasing doping level, both SDW and CDW show quasi-one dimensional like behavior, and the CDW has a period just half that of the SDW along one direction. From the calculation of the local density of states (LDOS), we found that the majority of the quasi-particles inside the vortex core are localized. All these results are consistent with several recent experiments on HTS.

PACS numbers: 74.20.-z, 74.25Jb, 74.60.Ec

Intensive efforts have been focused recently on the nature of vortex core excitations and the possible induction of SDW and other phases in the mixed state of high T_c superconductors (HTS). Experiments from the scanning tunneling microscope (STM) [1–3], neutron scattering [4–6] and nuclear magnetic resonance (NMR) [7] provided vital information on these topics. For example, according to the neutron scattering experiment by Lake *et al.* [5], a remarkable antiferromagnetism or SDW appears in the optimally doped $\text{La}_{2-x}\text{Sr}_x\text{CuO}_4$ when a strong magnetic field is applied. Very recently, STM measurement by Hoffman *et al.* [3] studied the LDOS in the mixed states of optimally doped $\text{Bi}_2\text{Sr}_2\text{CaCu}_2\text{O}_{8+\delta}$, and they found that associated with SDW, an inhomogeneous CDW exist both inside and outside the vortex cores. The coexistence of d -wave superconductivity (DSC) and SDW orders was theoretically studied by several groups in the absence of a magnetic field [8–11]. In the presence of a magnetic field, this problem was studied by the $\text{SO}(5)$ theory [12] and also by a Ginzburg-Landau approach [13]. The LDOS at the vortex core in a pure DSC were first calculated by authors in Ref.(14). With induced antiferromagnetic (AF) order, the LDOS was investigated without the contribution of the quasiparticles [12,13], and by a mean field study [15].

Although the competition between the SDW and DSC in a magnetic field was previously examined, the nature of the induced SDW and its spatial variation have not been addressed in such detail as to compare with the experiments. In this paper, we shall adopt the method described in previous papers [14,15] to examine the possible induction of extended SDW and CDW orders in the mixed state of HTS, and their nature in under-, optimally and overdoped samples. In order to simplify the numerical calculation, we shall assume a square vortex lattice for the mixed state and a strong magnetic field B such that $\lambda \gg b \gg \xi$ with λ as the London penetration depth, ξ the coherence length and b the vortex lattice constant. Under this condition, the applied magnetic field B can be

regarded as a constant throughout the sample. Our calculation is based upon an effective model Hamiltonian with competing SDW and DSC orderings. In the absence of a magnetic field B and for the optimally (hole) doped sample $x = 0.15$, the parameters are chosen in such a way that the SDW ordering is completely suppressed and only the DSC ordering prevails. When the system is in the mixed state driven by a magnetic field B , an inhomogeneous SDW is induced. We found that the structure of the induced SDW is determined and pinned by the underlying vortex lattice. For optimized doping sample, the modulation of the induced SDW and its associated CDW is determined by the vortex lattice and their patterns obey the four-fold symmetry. With the same set parameters and $B=0$, SDW, DSC and CDW stripes appear in the underdoped sample ($x = 0.12$). In the presence of a strong B , all order parameters pattern show remarkable anisotropic behavior along the x and y directions, and the CDW has a period just half that of the SDW along one direction. Increasing the SDW interaction strength can also lead to quasi-one dimensional pattern. The LDOS near the vortex core has also been calculated. It shows an asymmetric double peaks around $E = 0$ in agreement with the results of Ref.(15) and experiments [1,2]. In addition our results also show a small gap at $E = 0$ indicating the presence of the SDW order in the bulk sample. From the spatial profile of the LDOS, we conclude that almost all the quasiparticles inside the vortex core are localized.

Let us begin with a phenomenological model in which interactions describing both DSC and SDW order parameters in a two-dimensional lattice are considered. The effective Hamiltonian can be written as:

$$H = \sum_{\mathbf{i}, \mathbf{j}, \sigma} -t_{\mathbf{i}, \mathbf{j}} c_{\mathbf{i}\sigma}^\dagger c_{\mathbf{j}\sigma} + \sum_{\mathbf{i}, \sigma} (U n_{\mathbf{i}\bar{\sigma}} - \mu) c_{\mathbf{i}\sigma}^\dagger c_{\mathbf{i}\sigma} + \sum_{\mathbf{i}, \mathbf{j}} (\Delta_{\mathbf{i}, \mathbf{j}} c_{\mathbf{i}\uparrow}^\dagger c_{\mathbf{j}\downarrow}^\dagger + h.c.) . \quad (1)$$

The summation here is over the nearest neighbors sites. $c_{i\sigma}^\dagger$ is the electron creation operator and μ is the chemical potential. In the presence of magnetic field B , the hopping integral can be expressed as $t_{i,j} = t_0 e^{i\frac{\pi}{\Phi_0} \int_{\mathbf{r}_i}^{\mathbf{r}_j} \mathbf{A}(\mathbf{r}) \cdot d\mathbf{r}}$ for the nearest neighboring sites (i, j) . For simplicity, we have set the next-nearest neighbor hopping equal to zero. $\Phi_0 = h/2e$ is the superconducting flux quanta. Here we choose Landau gauge $\mathbf{A} = (-By, 0, 0)$ with y as the y -component of the position vector \mathbf{r} . The two possible orders in cuprates are SDW and DSC which have the following definitions respectively: $\Delta_i^{SDW} = U \langle c_{i\uparrow}^\dagger c_{i\uparrow} - c_{i\downarrow}^\dagger c_{i\downarrow} \rangle$ and $\Delta_{i,j} = V_{DSC} \langle c_{i\uparrow}^\dagger c_{j\downarrow} - c_{i\downarrow}^\dagger c_{j\uparrow} \rangle / 2$. In the above expressions, U and V_{DSC} are respectively the interaction strengths for SDW and DSC orders. The mean-field Hamiltonian (1) can be diagonalized by solving the resulting Bogoliubov-de Gennes equations self-consistently

$$\sum_j \begin{pmatrix} \mathcal{H}_{i,j} & \Delta_{i,j} \\ \Delta_{i,j}^* & -\mathcal{H}_{i,j}^* \end{pmatrix} \begin{pmatrix} u_j^n \\ v_j^n \end{pmatrix} = E_n \begin{pmatrix} u_i^n \\ v_i^n \end{pmatrix}, \quad (2)$$

where the single particle Hamiltonian $\mathcal{H}_{i,j}^\sigma = -t_{i,j} + (Un_{i\bar{\sigma}} - \mu)\delta_{ij}$, and

$$n_{i\uparrow} = \sum_n |u_i^n|^2 f(E_n), \quad (3)$$

$$n_{i\downarrow} = \sum_n |v_i^n|^2 (1 - f(E_n)), \quad (4)$$

$$\Delta_{i,j} = \frac{V_{DSC}}{4} \sum_n (u_i^n v_j^{n*} + v_i^{n*} u_j^n) \tanh\left(\frac{E_n}{2k_B T}\right), \quad (5)$$

with $f(E)$ as the Fermi distribution function and the electron density $n_i = n_{i\uparrow} + n_{i\downarrow}$. The DSC order parameter at each site i is $\Delta_i^D = (\Delta_{i+\mathbf{e}_x, i}^D + \Delta_{i-\mathbf{e}_x, i}^D - \Delta_{i, i+\mathbf{e}_y}^D - \Delta_{i, i-\mathbf{e}_y}^D) / 4$ where $\Delta_{i,j}^D = \Delta_{i,j} \exp[i\frac{\pi}{\Phi_0} \int_{\mathbf{r}_i}^{\mathbf{r}_j} \mathbf{A}(\mathbf{r}) \cdot d\mathbf{r}]$ and $\mathbf{e}_{x,y}$ denotes the unit vector along (x, y) direction. The main procedure of self-consistent calculation is given below: For a given initial set of parameters $n_{i\sigma}$ and $\Delta_{i,j}$, the Hamiltonian is numerically diagonalized and the electron wave functions obtained are used to calculate the new parameters for the next iteration step. The calculation is repeated until the relative difference of order parameter between two consecutive iteration step is less than 10^{-4} . The solutions corresponding to various doping concentrations can be obtained by varying the chemical potential.

In the following calculation, the length and energy are measured in units of the lattice constant a and the hopping integral t_0 respectively. We need to point out that the induction of internal magnetic field by the supercurrent around the vortex core is so small comparing with the external magnetic field that we can safely adopt the

uniform magnetic field distribution approximation. We follow the standard procedures [14,15] to introduce magnetic unit cells, where each unit cell accommodates two superconducting flux quanta. By introducing the quasi-momentum of the magnetic Bloch state, we obtain the wave function under the periodic boundary condition whose region covers many unit cells. The related parameters are chosen as the following: The DSC coupling strength is $V_{DSC} = 1.2$, the linear dimension of the unit cell of the vortex lattice is chosen as $N_x \times N_y = 40 \times 20$ sites and the number of the unit cells $M_x \times M_y = 20 \times 40$. This choice corresponds the magnetic field $B \simeq 37T$.

At optimal doping and $B = 0$, the important qualitative characteristic of the quasiparticle states is identical to that of a pure d-wave superconductor. At the first step, the magnitudes of parameters are selected to fulfill such requirement that the AF order is completely suppressed and only DSC prevails in the absence of a magnetic field. Here we choose the hole doping $x = 0.15$ and $U = 2.4$. Our calculation is performed at very low temperature where the vortex structure is almost independent of temperature. In Fig. 1(a) we plot the typical configuration of vortex structure. The DSC order parameter vanishes at the vortex core center and recovers its bulk value at a couple of coherence lengths away from the center. By comparing it with the vortex structure of a pure DSC, the size of the vortex core here is noticed to be enlarged. The centers of the two vortex cores are at sites (10, 10) and (30, 10). Fig. 1(b) displays the spatial distribution of the staggered magnetization of the induced SDW order as defined by $M_i^s = (-1)^i \Delta_i^{SDW} / U$. It is obvious that the AF order exists both inside and outside the vortex cores, and behaves like a two-dimensional SDW with the same wave length in the x and y directions. The induced SDW order reaches its maximum value at the vortex core center and the magnitude of its spatial variation still holds the fourfold symmetry as that of the pure DSC case. The order of DSC and SDW coexist throughout the whole sample. The appearance of the SDW order around the vortex cores strongly affects the spatial profile of the local electron density distribution, which can be represented by a weak CDW as shown in Fig. 1(c). The remarkable enhancement of electron density (or depletion of the hole density) is presented at the vortex core center. It is easy to observe that the four-fold symmetry holds for both SDW and CDW with the same wavelength $20a$.

To have a deeper understanding of the above results, the case of an underdoped sample ($x = 0.12$) is examined. After the calculation is performed at $B = 0$, we found that DSC, SDW and CDW orderings have the stripe structures, which is consistent with stripe phase results reported by Martin *et al.* [11]. We have compared the free energy between stripe phase solution with a uniform AF solution and found that the free energy of the stripe phase is always lower. In the presence of a strong

magnetic field B , the profile of DSC order parameter is shown in Fig. 2(a). The radius of vortex is further enlarged than in Fig. 1(a). The qualitative features of Fig. 2 are quite different from those in Fig.1 and the spatial variation of the SDW becomes quasi-one dimensional. Its periods of oscillations are fixed by the vortex lattice similar to the case of $x = 0.15$. We also noticed that the AF order is much enhanced in the mixed state as compared with its values in the stripe phase at $B = 0$, in agreement with Katano's experiment [4]. The results are presented in Fig. 2(b) and Fig. 2(c), where the anisotropy in the magnitudes of SDW and CDW along the x and y directions shows quasi-one-dimensional behavior. The periods of SDW and CDW are respectively $20a$ and $10a$. These results are in qualitative agreement with the observations of Lake *et al.* [6] where a magnetic field induced striped AF order was observed in underdoped sample. We also have calculated the case for overdoped sample ($x = 0.20$) with the same set of parameters. For $B = 0$, the SDW order is completely suppressed and the DSC order is homogeneous in real space. When B is strong, the SDW order does not show up even inside the vortex core.

We notice that the periods of SDW and CDW obtained from the experiments [3,5] are respectively $8a$ and $4a$ for optimal doping sample. With the present band parameters, we are not able to obtain these numbers. However, the experimental values could be obtained by tuning U , doping or including a next-nearest neighbor hopping term. For larger U case, the configurations of SDW and CDW exhibit stripe-like behavior along the x - (or y -) direction. The periodicity of CDW is always half that of SDW. For example when $U = 3$ and $x = 0.20$, the periodicity of SDW and CDW are respectively $10a$ and $5a$. But under this condition, the AF stripe phase would appear in the optimally doped sample.

Next we present the calculation of the LDOS near the center of vortex core for hole doping $x = 0.15$. The LDOS is given by:

$$\rho_i(E) = - \sum_n [|u_i^n|^2 f'(E_n - E) + |v_i^n|^2 f'(E_n + E)], \quad (6)$$

It also measures the differential tunnel conductance, which could be measured by STM experiments. In this case, the thermally broadening effect has not been considered here and the temperature is fixed at $T = 0.01$. We plot the LDOS at the core center vs the quasi-particle energy measured from the Fermi level. For comparison, we have also displayed the LDOS at the site between two next-nearest neighboring vortex cores. The results are shown in Fig. 3. At the core center, the coherent peaks due to the gap edges of the superconductor at $B = 0$ are suppressed, and two asymmetric peaks of the vortex states appear slightly above and below $E = 0$. The spectrum agrees qualitatively with the experiment for YBCO [1], and that of Ref.(15). But a closer inspection reveals that the distance between these two peaks

becomes slightly larger than that in Ref.(15). The peak at about $E = 0.8$ seems to be the characteristic of the bulk SDW order and the band structure effect. It is easy to notice that the magnitude of the LDOS at $E = 0$ approaches zero which indicates a bulk SDW gap. From the spatial distribution of LDOS at $E = 0$ (see Fig. 4(a)), we find that LDOS is enhanced along the $x = y$ and $x = -y$ or the diagonal directions from the center of the vortex core. This 'star'-like behavior indicates the small number of quasiparticles very close to $E = 0$ are extended [16]. We also present the result (see Fig. 4(b)) for the peak on the left of $E = 0$ in Fig. 3. Its profile displays an obvious localized shape even though it decays somewhat slower along the x and y directions than the diagonal directions. The peak on the right at $E \simeq 0.16$ has a similar spatial distribution which is not shown here. From Fig. 4(b), we conclude that the majority of quasiparticles inside the vortex core with energies near or at the two asymmetric peaks are in fact localized, in agreement with experiments [3,5].

In conclusion, we have studied the induction of SDW and CDW orders in optimally and underdoped HTS by a strong magnetic field. Consider only the nearest neighbor hopping term, the spatial variations of DSC, SDW and CDW orders have been numerically presented in Fig. 1 and Fig. 2 and stripe-like structure exhibits for underdoped sample. The LDOS near the vortex center have also been calculated. We show that almost all the quasiparticles inside the core are localized, that is very different from case for a pure DSC vortex [16]. These results are consistent with recent STM, neutron scattering and NMR experiments on HTS. Finally we would like to emphasize that although our self-consistent BdG calculation based upon a mean-field approach tends to overestimate the stability of the SDW phase, the qualitative features of our results should still be valid, particularly in view of their favorable comparisons with experiments.

We are grateful to Dr. J.-X. Zhu and Prof. S. H. Pan for useful discussion and Prof. J. C. Davis for showing us the results of Ref.(3) before its publication. This work was supported by a grant from the Robert A. Welch Foundation and by the Texas Center for Superconductivity at the University of Houston through the State of Texas, and by a Texas ARP grant(003652-0241-1999).

-
- [1] I. Maggio-Aprile *et al.*, Phys. Rev. Lett. **75**, 2754 (1995).
 - [2] S. H. Pan *et al.*, Phys. Rev. Lett. **85**, 1536 (2000).
 - [3] J. E. Hoffman *et al.*, Science **295**, 466 (2002).
 - [4] S. Katano *et al.*, Phys. Rev. B. **62**, R14677 (2000).
 - [5] B. Lake *et al.*, Science **291**, 1759 (2001); B. Lake *et al.*, cond-mat/0104026.

- [6] B. Lake *et al.*, Nature **415**, 299 (2002).
- [7] V. F. Mitrovic *et al.*, Nature **413**, 501 (2001).
- [8] V. J. Emery and S. A. Kivelson, Nature **374**, 434 (1995); V. J. Emery, S. A. Kivelson, and J. M. Tranquada, Proc. Natl. Acad. Sci. USA **96**, 8814 (1999);
- [9] L. Balents, M. P. A. Fisher, and C. Nayak, Int. J. Mod. Phys. B **12**, 1033 (1998).
- [10] Bumsoo Kyung, Phys. Rev. B. **62**, 9083 (2000).
- [11] I. Martin, *et al.*, Int. J. Mod. Phys. B **14**, 3567 (2000).
- [12] D. P. Arovas *et al.*, Phys. Rev. Lett. **79**, 2871 (1997); J. -P. Hu, and S. C. Zhang, cond-mat/0108273.
- [13] E. Demler, S. Sachdev, and Y. Zhang, Phys. Rev. Lett. **87**, 067202 (2001); A. Polkovnikov, *et al.*, cond-mat/0110329.
- [14] Y. Wang and A. H. MacDonald, Phys. Rev. B **52**, R3876 (1995).
- [15] Jian-Xin Zhu, and C. S. Ting, Phys. Rev. Lett. **87**, 147002 (2001).
- [16] Jian-Xin Zhu, C. S. Ting, and A. V. Balatsky, cond-mat/0109503.

FIG. 1. The amplitude distribution of the DSC order parameter Δ_i^D (a), the staggered magnetization M_i^s (b), and the electron density n_i (c) in one magnetic unit cell. The size of the cell is 40×20 , corresponding to a magnetic field $H = \Phi_0/(20 \times 20)$. The strength of the on-site repulsion $U = 2.4$ and the averaged electron density $\bar{n} = 0.85$.

FIG. 2. The amplitude of the DSC order parameter Δ_i^D (a), the staggered magnetization M_i (b), and the electron density n_i (c) in one magnetic unit cell. The averaged electron density $\bar{n} = 0.88$. The other parameter values are the same as Fig. 1.

FIG. 3. Quasiparticle LDOS profiles at the center of the vortex core are shown by solid lines. The dashed lines show the LDOS at the site midway between two next-nearest neighbor vortices. The averaged electron density $\bar{n} = 0.85$.

FIG. 4. The spatial distribution of LDOS in a vortex unit cell at the energy $E = 0$ a) and $E = -0.126$ (b).

Fig.1(a) Chen & Ting

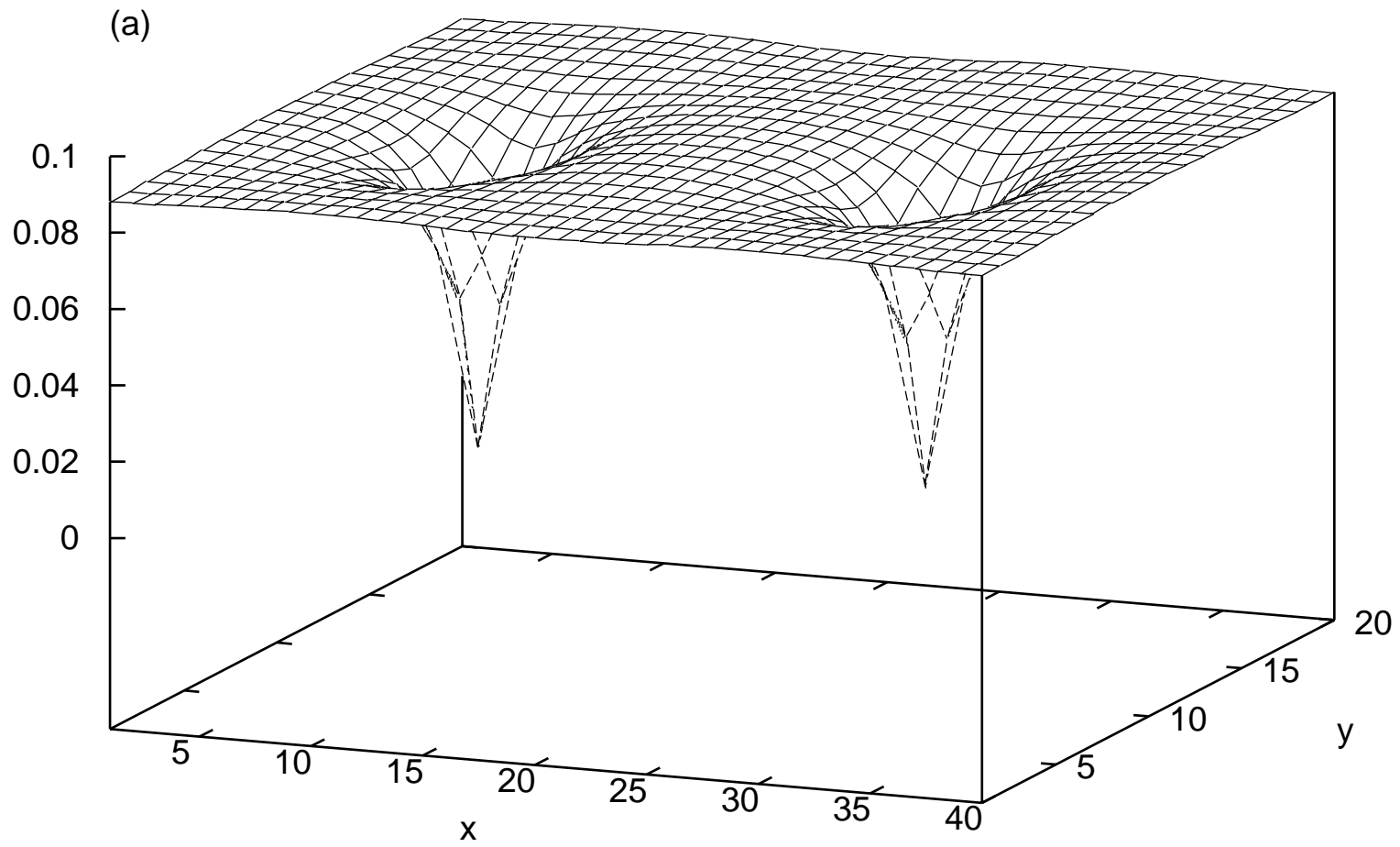


Fig.1(b) Chen & Ting

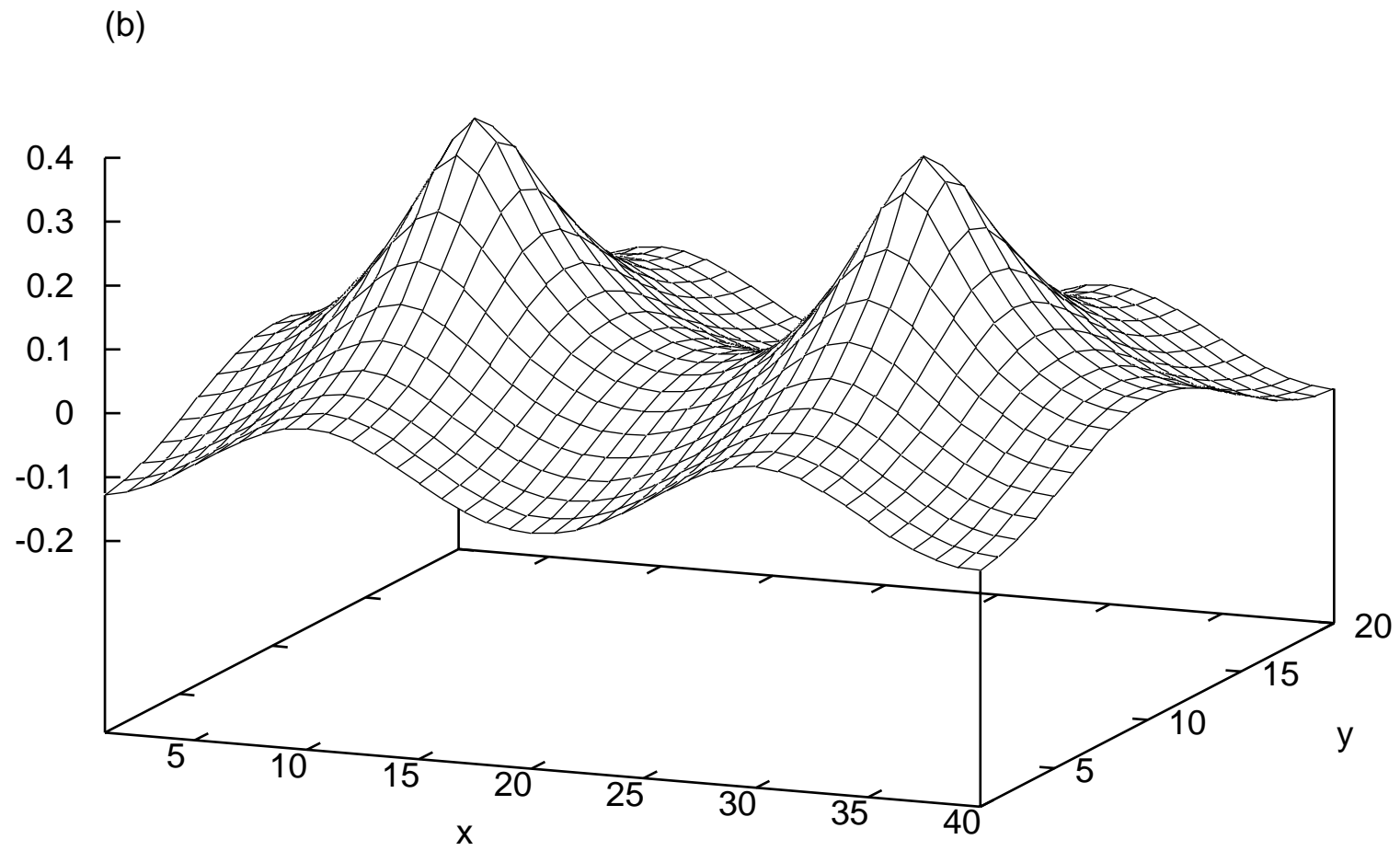


Fig.1(c) Chen & Ting

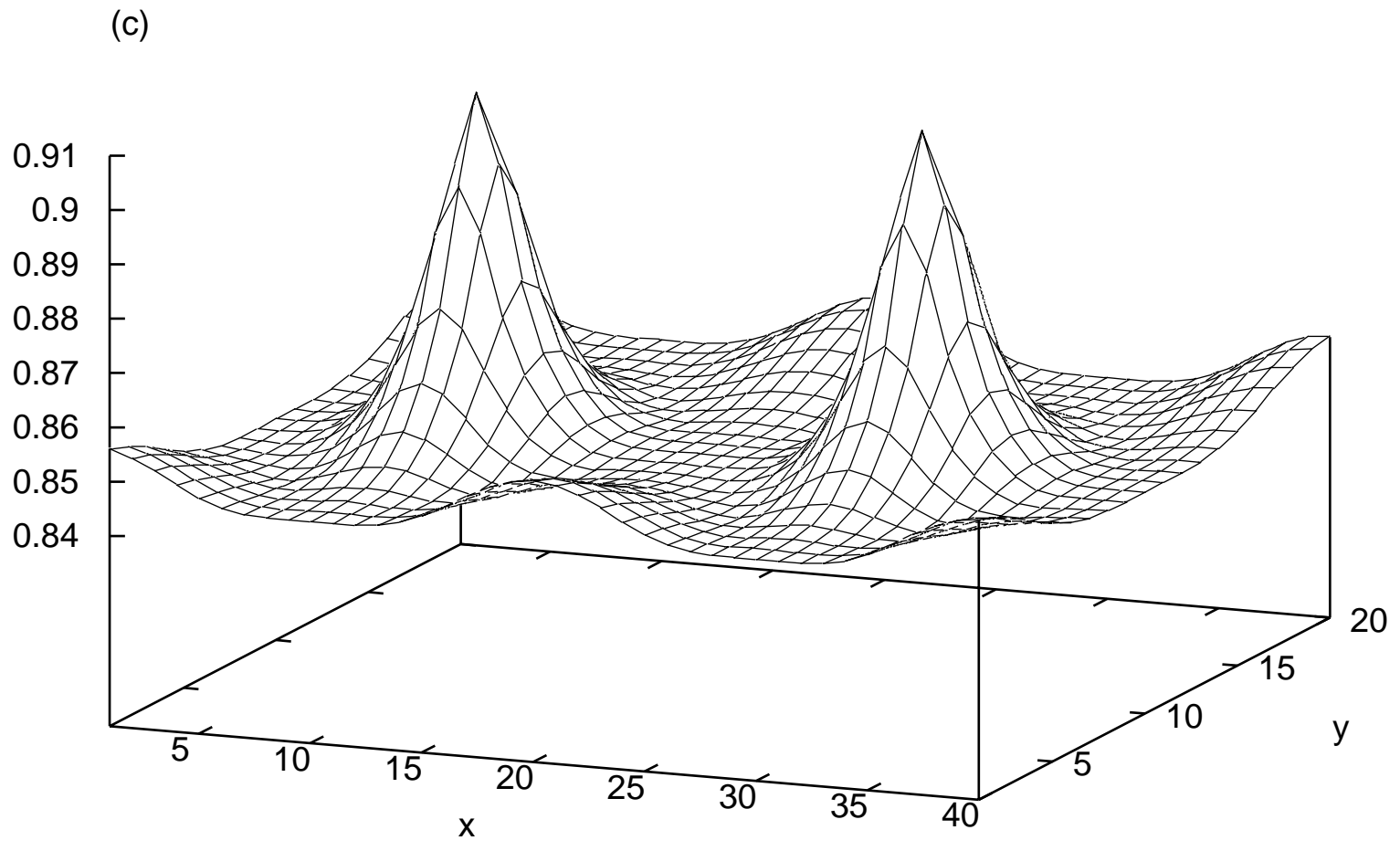


Fig.2(a) Chen & Ting

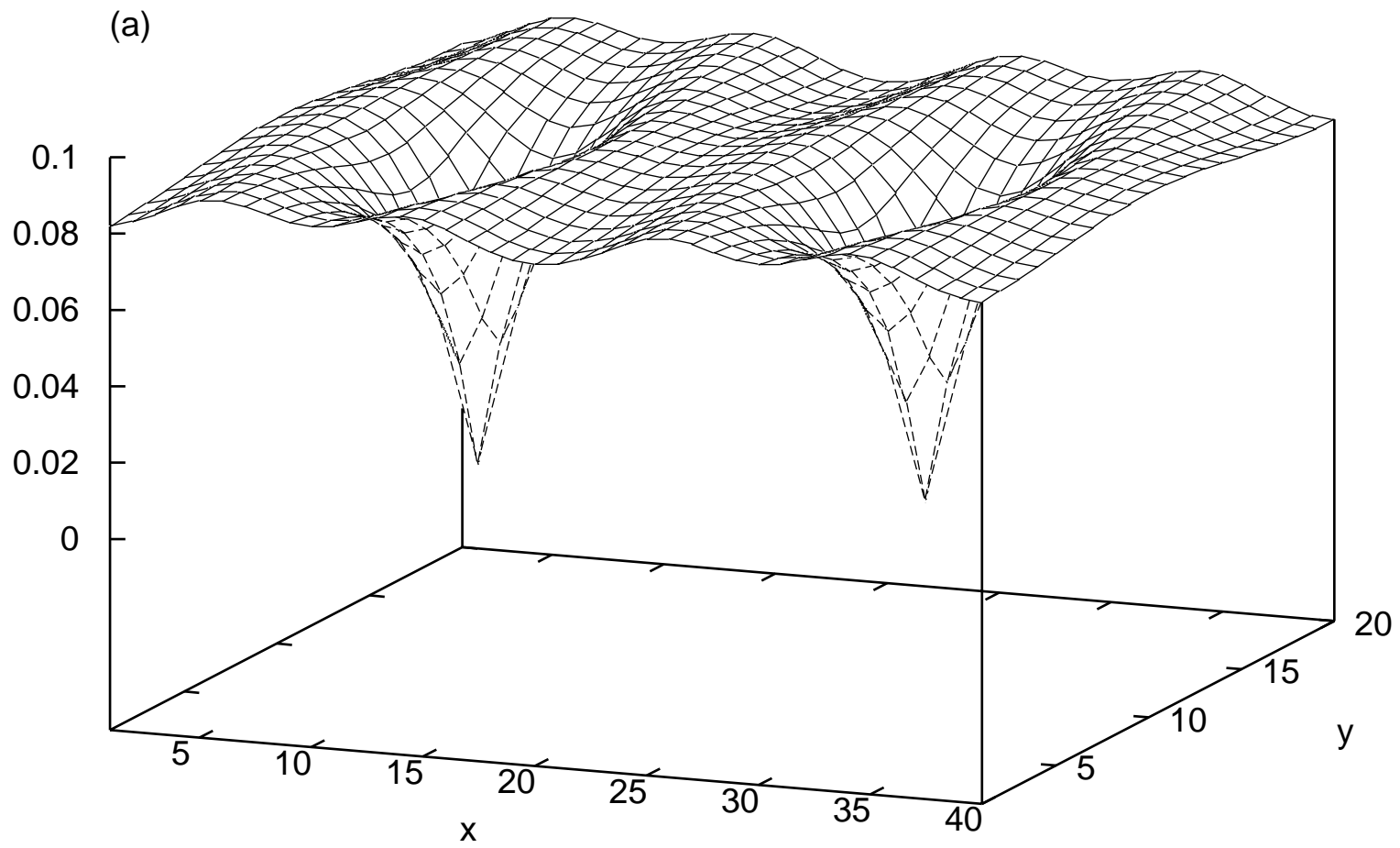


Fig.2(b) Chen & Ting

(b)

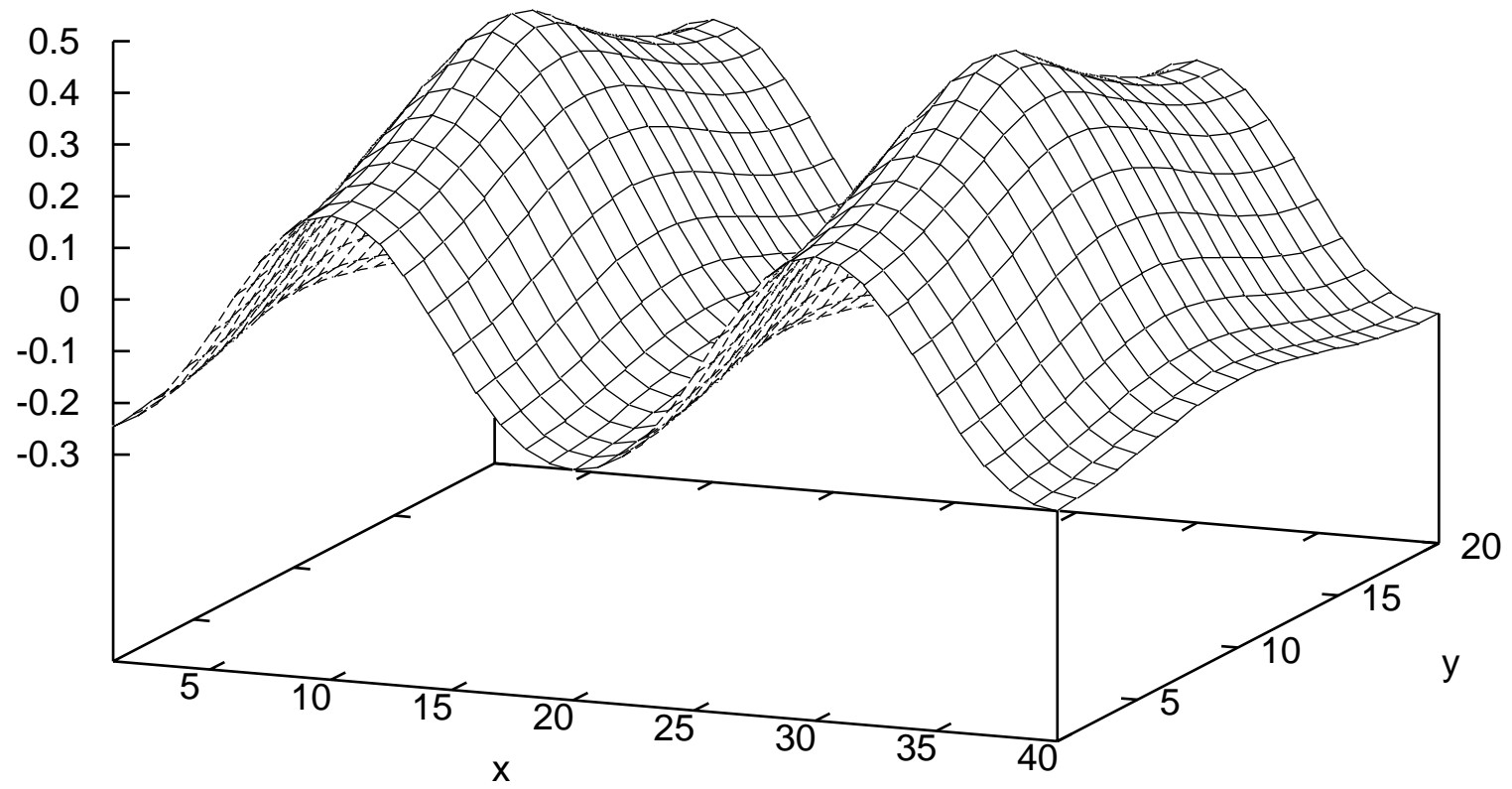


Fig.2(c) Chen & Ting

(c)

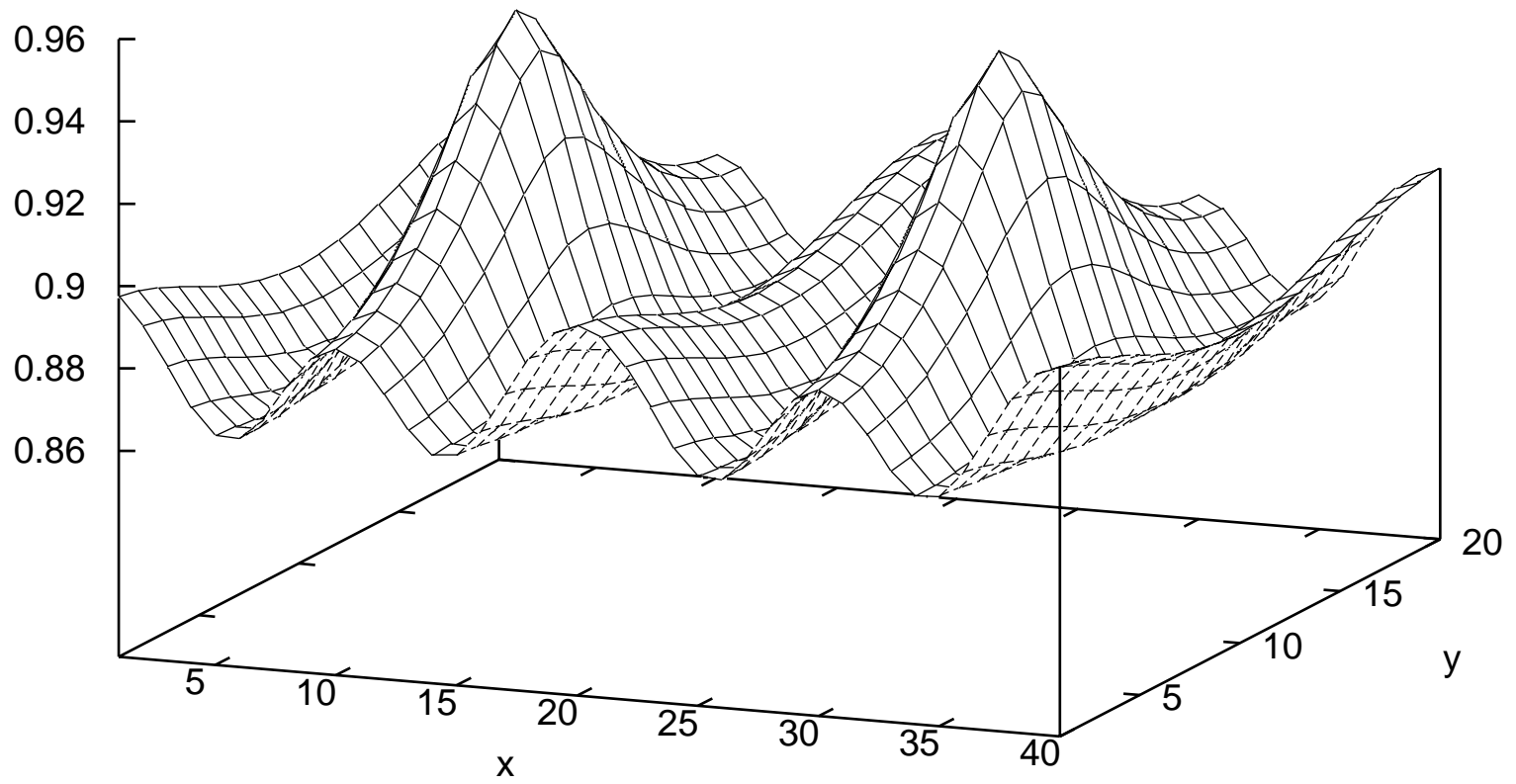


Fig.3 Chen & Ting

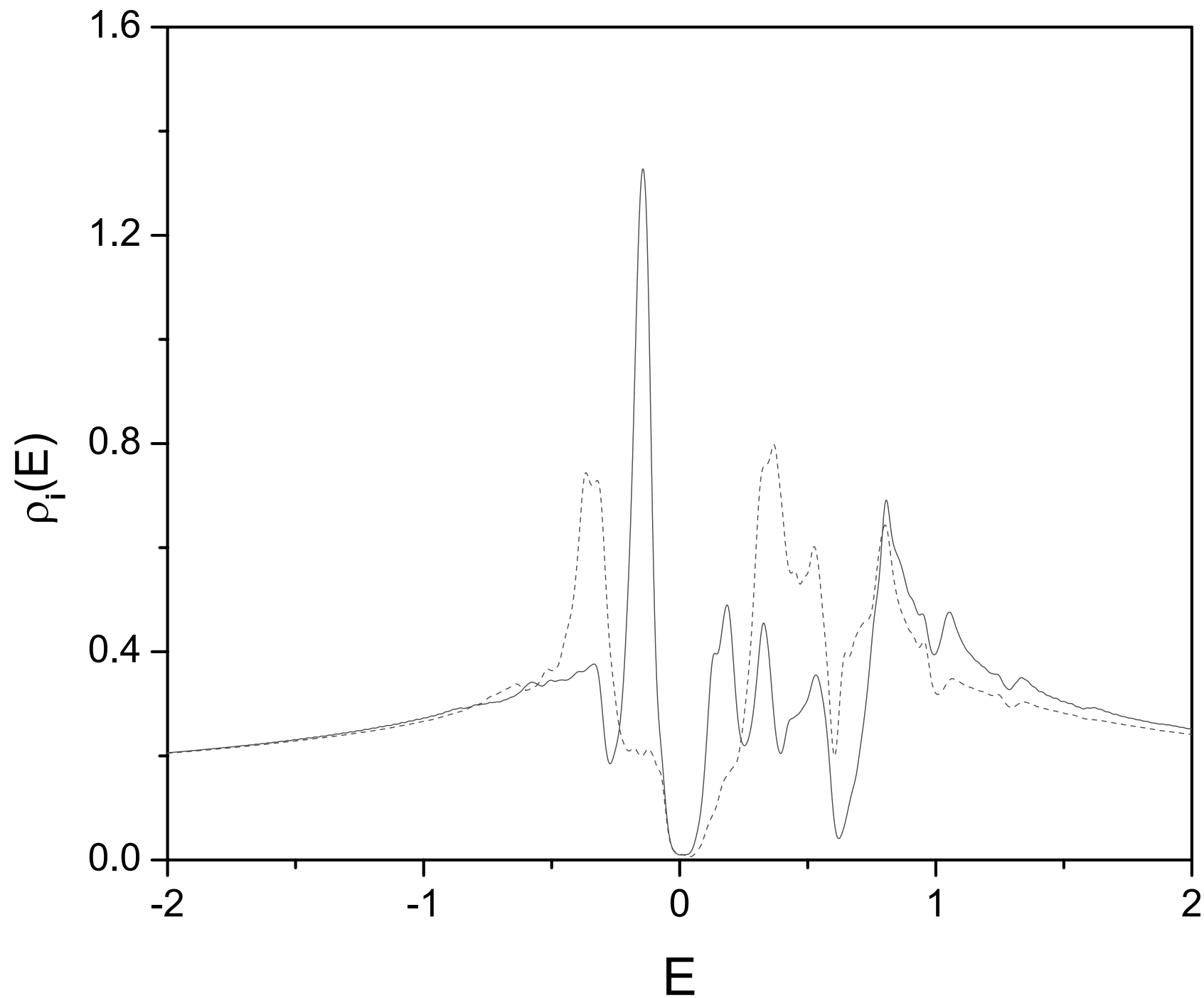


Fig.4(a) Chen & Ting

(a)

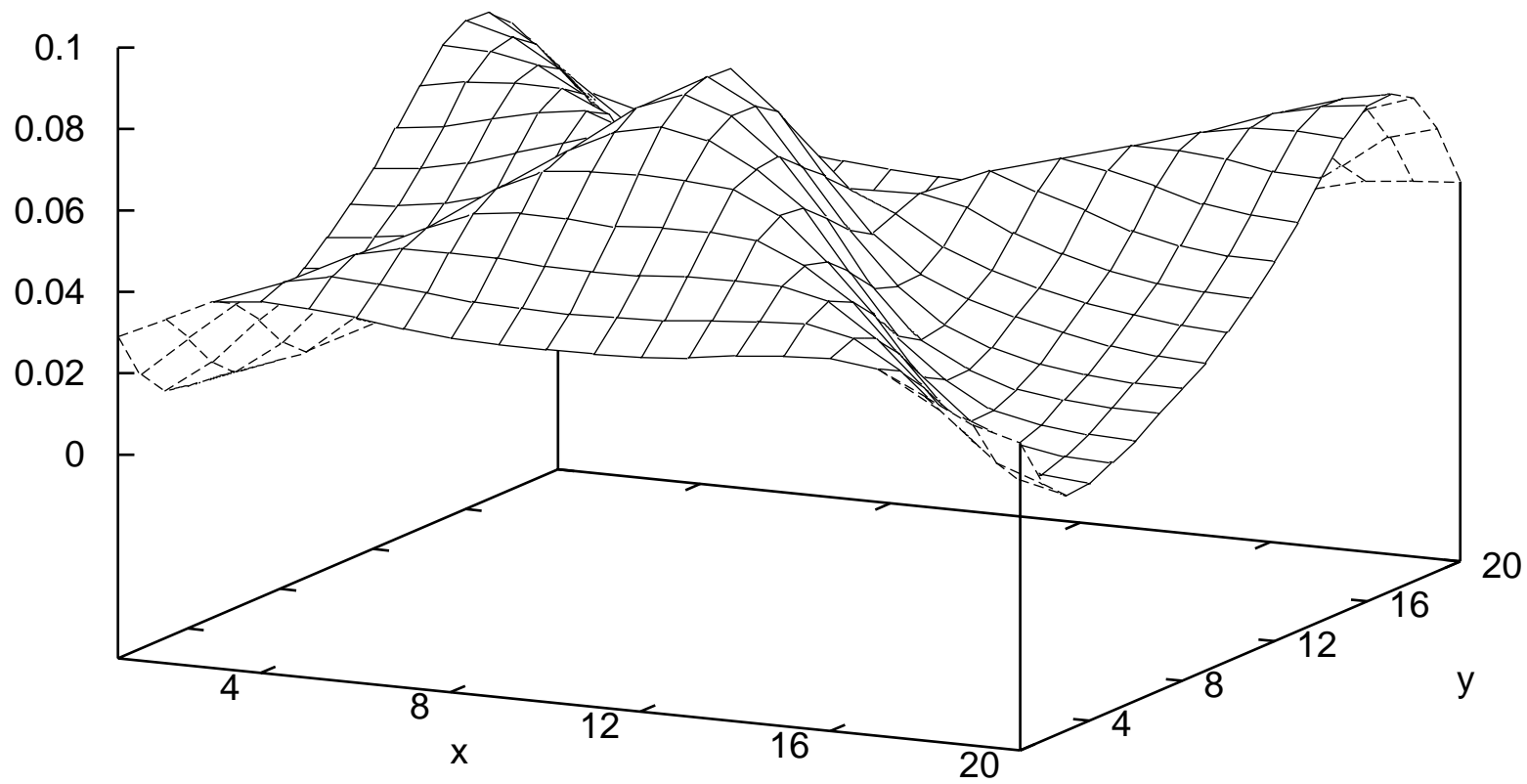


Fig.4(b) Chen & Ting

(b)

